Anisotropy of Optical Phonons in GaAs-AlAs Superlattices

Shang-Fen Ren, Hanyou Chu, and Yia-Chung Chang
Department of Physics and Materials Research Laboratory, University of Illinois at Urbana-Champaign, Urbana, Illinois 61801
(Received 3 August 1987)

Phonon dispersion curves of GaAs-AlAs superlattices for various directions of propagation are examined with a detailed microscopic model which takes into account the long-range Coulomb interaction. The anisotropy of the long-wavelength optical modes and its relation with the interface modes are studied. Our theoretical predictions are in accord with the experimental data.

PACS numbers: 63.20.Dj, 78.30.Fs

Recently, extensive studies of phonons in GaAs-AlAs superlattices have been reported.[1-7] Although the measured phonon frequencies for acoustical modes are well described by several theoretical models, the existing experimental data for optical modes are less well understood. The anisotropy of optical phonons in materials with wurtzite structures was previously observed.[8,9] Similar anisotropic behavior of the long-wavelength principal optical phonons in GaAs-AlAs superlattices was observed by Merlin *et al.*[1] They found that these principal optical modes exhibit two distinct frequencies when they propagate along the growth direction and along the in-plane direction (parallel to the interface). Their results are consistent with the theoretical predictions based on Rytov's macroscopic model.[10] In superlattices, there also exist some interface modes[11] which reduce to the principal optical modes with in-plane propagation in the long-wavelength limit. Such interface modes have been observed by Sood *et al.*[12] In this Letter we report theoretical calculations of phonon dispersion curves of GaAs-AlAs superlattices based on an eleven-parameter rigid-ion model.[13,14] We show that the anisotropic behavior of optical modes in superlattices can be well accounted for by our microscopic model. By examining the phonon dispersion curves for wave vectors parallel to the interface, we find that the in-plane optical modes (due to anisotropy) observed by Merlin *et al.*[1] and the interface modes observed by Sood *et al.*[12] are closely related.

The eleven-parameter rigid-ion model[13,14] has been used successfully to calculate phonon dispersion curves in bulk materials. Here we use this model to describe superlattices. For convenience of later discussion, we define an atomic layer as a collection of atoms in a plane normal to the growth direction, a bilayer as two adjacent atomic layers, and a sublattice as a collection of all equivalent atomic layers (one in each period) of the superlattice. The parameters of GaAs are taken from Kunc,[13] and the parameters of AlAs are fitted to the existing experimental data.[2,4,15]

The dynamic matrix for the superlattice $\mathbf{C}(\mathbf{k})$ consists of two parts—the short-range interaction $\mathbf{C}^{\mathrm{sr}}(\mathbf{k})$ and the long-range Coulomb interaction $\mathbf{C}^{\mathrm{C}}(\mathbf{k})$. For the short-range part, interactions up to the second neighbor are included. Short-range interaction parameters between any two atoms in the superlattice are taken to be the same as in the corresponding bulk material, except that the interaction between a Ga atom and an Al atom across an interface is taken to be the average of the Ga-Ga interaction in bulk GaAs and the Al-Al interaction in bulk AlAs.

The long-range Coulomb interaction is important for zinc-blende materials since it gives rise to a sizable splitting of the longitudinal- and transverse-optical modes at the zone center. The fundamental theory on how to include the long-range Coulomb interaction for bulk crystals was previously documented.[16-18] However, it is more difficult to calculate the long-range Coulomb terms in the superlattice because of its low symmetry. For calculating Coulomb interactions between sublattices, we adopt a method similar to that used by Yip and Chang,[5] but modified to ensure the convergence of the summations involved. In the present calculation the long-range Coulomb interaction is included exactly (i.e., summed over an infinite number of neighbors), whereas in Ref. 5 it was included by a perturbational method. For examination of the anisotropic behavior and the in-plane dispersion of phonons it is crucial to calculate the Coulomb interaction up to infinite distance. Details of the calculation will be presented elsewhere.[19] The final results for the Coulomb interaction between the lth and the l'th sublattices as $\mathbf{k}\rightarrow\mathbf{0}$ can be written as

$$C^{\mathrm{C}}_{i,j}(\mathbf{k},l,l')=\frac{4\pi Q_l Q_{l'}}{N_p}\frac{k_i k_j}{k^2}+D^{\mathrm{C}}_{i,j}(l,l'), \tag{1}$$

where i and j indicate the x, y, and z directions, Q_l and $Q_{l'}$ represent atomic-transfer charges of atoms in the lth and the l'th sublattices, respectively, and $l,l'=1,2,\ldots,2N_p$, where N_p is the total number of bilayers in a period. The irregular function $(k_i k_j/k^2)$ in the first term has different values when $\mathbf{k}$ approaches zero from different directions. The second term $D^{\mathrm{C}}_{i,j}(l,l')$ on the right-hand side is direction independent. This result is similar to that obtained in a bulk system, except that here $D^{\mathrm{C}}_{i,j}$ does not have the cubic symmetry, so it cannot be reduced to an identity matrix multiplied by a con-

stant.

In our calculations, the bulk GaAs electron-transfer charge Q_a is used for inner GaAs layers, and the bulk AlAs electron-transfer charge Q_b for inner AlAs layers. At interfaces, the transfer charge of As is taken as the average of Q_a and Q_b since the electron overlapping is significant only for the nearest neighbors.

The short-range interaction matrix between sublattices l and l' at $k=0$ can be similarly written as $D_{i,j}^{\mathrm{sr}}(l,l')$ and it is easy to show that $D_{i,j}^{\mathrm{C}}$ and $D_{i,j}^{\mathrm{sr}}$ have the same symmetry property. As demonstrated previously,[16,18] it is the irregular $(k_i k_j/k^2)$ term that accounts for the anisotropic behavior in uniaxial crystals. Similar to the case in bulk uniaxial crystal, the superlattice system can exhibit different optical-phonon frequencies for $\mathbf{k}$ approaching zero from different directions. This can be understood as follows. For a superlattice system, the direction-independent term $D_{i,j}^{\mathrm{sr}}+D_{i,j}^{\mathrm{C}}$ in the dynamic matrix at $\mathbf{k}=\mathbf{0}$ has the following form:

$$\begin{pmatrix} a & b & 0 \\ b & a & 0 \\ 0 & 0 & c \end{pmatrix}.$$

When the direction-dependent terms $k_i k_j/k^2$ are added on, the phonon frequencies for the superlattice at $\mathbf{k}=\mathbf{0}$ become angular dependent. For bulk cubic crystals, the direction-independent term at $\mathbf{k}=\mathbf{0}$ has a diagonal form which remains unchanged when we rotate the coordinate system. Thus, the phonon frequencies at $\mathbf{k}=\mathbf{0}$ are angular independent.

As an example, the dispersion curves for phonons in a $(GaAs)_5(AlAs)_4$ superlattice are shown in Fig. 1 along the growth direction ([001]) and along the [100] (in-plane) direction. We first examine the phonon modes along the [001] direction. The top eight lines between 10–12 THz are AlAs-like optical modes, and the next ten lines between 7–9 THz are GaAs-like optical modes. Here, solid curves denote transverse modes (doubly degenerate) and dashed curves denote longitudinal modes. All optical modes are nearly dispersionless as they are well confined either in the GaAs or AlAs slabs. The phonon modes with frequencies below 7 THz are all derived from acoustical branches. The superlattice acoustical modes are mixtures of GaAs and AlAs acoustical modes and several minigaps appear at the zone center and zone boundary as a result of the dissimilarity between GaAs and AlAs.

We next examine the phonon modes along the [001] direction. In this direction, all the degeneracies disappear, so the top twelve lines are AlAs-like optical modes, and the next fifteen lines are GaAs-like optical modes. The lower-lying curves are again GaAs-AlAs mixed acoustical modes. As can be seen in Fig. 1 for certain optical modes, the frequencies at the zone center (Γ) are different when $\mathbf{k}\rightarrow\mathbf{0}$ from different directions, clearly indicating an anisotropic behavior. The four optical

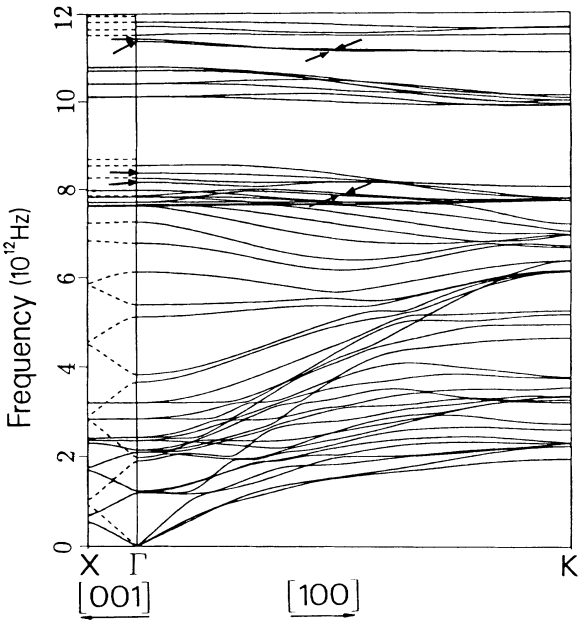

FIG. 1. Phonon dispersion curves for a $(GaAs)_5(AlAs)_4$ superlattice along the growth direction ([001]) and the [100] direction.

modes marked by arrows at Γ correspond to (from top to bottom) the principal LO (AlAs), TO (AlAs), LO (GaAs), and TO (GaAs) modes with in-plane propagation. By comparing the in-plane dispersion curves with the projected phonon bands for bulk GaAs and AlAs, we can also identify the interface modes. The projected phonon bands are families of phonon dispersion curves along the in-plane direction with arbitrary values of k_z (wave vector along the [001] direction) for bulk materials. The superposition of the GaAs and AlAs projected phonon bands is shown in Fig. 2. Any phonon mode shown in the right panel of Fig. 1 which falls outside the projected phonon bands in Fig. 2 is an interface mode. For example, the modes marked by arrows at finite in-plane wave vectors in Fig. 1 are interface modes. In Fig. 1, we see that the two AlAs-like principal modes are in fact interface modes for all wave vectors along the in-plane direction. The two GaAs-like principal modes turn into interface modes for k_x between $0.3(2\pi/a)$ and $0.8(2\pi/a)$, a being the lattice constant. However, the relation between the GaAs-like principal modes and interface modes is obscured as a result of the interaction with other confined modes (see Fig. 1). Other interface modes can also be identified by a comparison of Figs. 1 and 2, but they are irrelevant to the central theme of this paper.

In Fig. 3, we plot the frequencies of optical modes at the zone center as functions of θ, the angle of the wave vector $\mathbf{k}$ measured from the growth direction. θ goes from 0 to $\pi/2$ as $\mathbf{k}$ goes from [001] to [100] in a plane

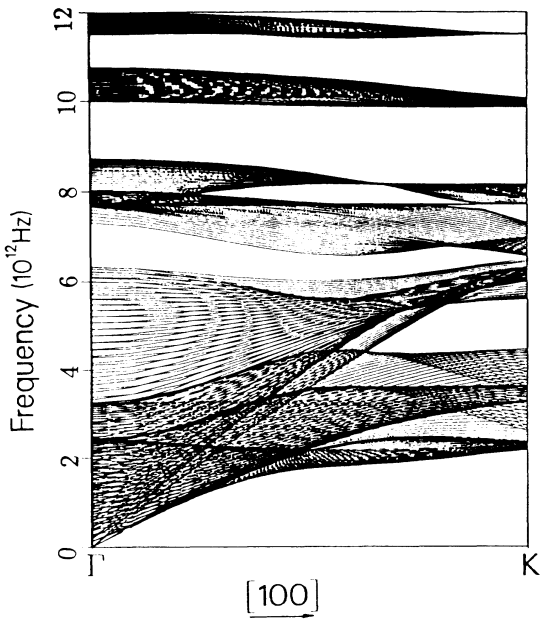

FIG. 2. Superposition of projected phonon bands for bulk GaAs and AlAs along the [100] direction.

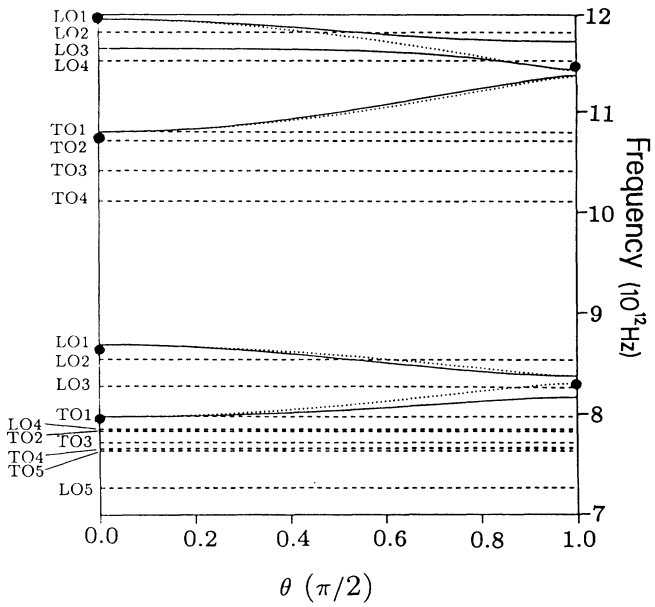

FIG. 3. Zone-center optical-phonon frequencies of a $(GaAs)_5(AlAs)_4$ superlattice plotted as functions of the direction of wave vector.

normal to [010]. For superlattice phonons derived from the acoustical modes, no obvious angular dispersions are observed and they are omitted for clarity. The solid lines denote modes with large angular dispersion and the dashed lines represent modes with weak or zero angular dispersion. The dotted lines are results obtained with a simple phenomenological model, which produces results essentially identical to those of Rytov's model.[10] Details of the phenomenological model will be discussed elsewhere.[19] The symbols LOn and TOn designate the nth quantized modes derived from bulk (AlAs or GaAs) LO and TO branches, respectively. Here n is the principal quantum number which is related to the number of nodes of the vibrational amplitude in a given mode. Note that the labels LOn and TOn are meaningful only at $\theta=0$, since at finite values of θ modes with different n's are mixed.

In Fig. 3, we see that only the $n=1$ modes can have gnificant angular dispersion; the other modes are essentially dispersionless except when they are mixed with an $n=1$ mode at some finite θ, where their frequencies tend to cross each other. For example, the AlAs-like LO1 and LO3 modes interact with each other for θ near $0.7(\pi/2)$; thus, the LO3 mode appears to have a significant angular dispersion. For $\theta>0.7(\pi/2)$, the mode labeled by LO3 is actually LO1-like. Similarly, the GaAs-like LO1 and LO3 modes interact at θ near $\pi/2$. Note that because the superlattice has reflection symmetry about a plane (normal to [001]) through the center of the GaAs or AlAs slabs, modes of even n and modes of odd n cannot mix. The magnitude of the angular dispersion is determined by the total dipole moment in a given superlattice mode [see the irregular term in Eq. (1)]. The dipole moment in a superlattice mode is approximately equal to the sum of dipole moments of all the bilayers in each period weighted by the superlattice envelope function. For $n=1$ modes the envelope function is positive everywhere; thus the total dipole moment is large. For the other modes the envelope function oscillates within a period and the net dipole moment is nearly zero. With the same argument, we can also understand why the superlattice modes derived from acoustical branches have almost no angular dispersion, since the dipole moment of a bilayer for acoustical modes is nearly zero.

Results of room-temperature Raman scattering measurements of Merlin *et al.*[1] are shown by filled circles in Fig. 3. Because the Raman intensity in this particular experiment is proportional to the dipole moment, only the $n=1$ modes have sufficient strengths to be observed. The agreement of our calculation with the experimental data is very good. The datum for the GaAs-like LO1 mode at $\theta=\pi/2$ falls between our predicted LO1 and LO3 modes. Because these two modes are strongly mixed, the Raman scattering spectrum may contain the superposition of the signals contributed from both modes. We have also examined the $(GaAs)_{18}$-$(AlAs)_{18}$ superlattice. The results compare favorably with the corresponding data (the 50–50-Å case) in Ref. 1. We find that the frequencies of the AlAs- and the GaAs-like LO1 modes at $\theta=\pi/2$ are 11.41 and 8.30 THz, respectively, while the experimental data are approximately

11.3 and 8.36 THz.

Sood *et al.*[12] performed resonant Raman scattering experiments on a number of GaAs-AlAs superlattices and observed the interface modes. We have also calculated the phonon dispersion curves for all in-plane wave vectors in the [100] direction for the $(GaAs)_7$-$(AlAs)_7$ and $(GaAs)_7$-$(AlAs)_{20}$ superlattices which correspond to samples A and B, respectively, in Ref. 12. We find that the interface mode frequencies are insensitive to the number of GaAs or AlAs bilayers within each period (N_1 or N_2) as long as both N_1 and N_2 are large enough (≥ 4). Thus, their dispersion curves look just like those marked with arrows shown in Fig. 1. The GaAs interface mode frequencies range from 7.8 to 8.05 THz for k_x from $0.8(2\pi/a)$ to $0.3(2\pi/a)$ and they turn into the principal modes at smaller k_x where their frequencies become dependent on N_1 and N_2. The interface modes observed by Sood *et al.*[12] in both these samples are peaked around 278 cm^{-1}, which correspond to 268 cm^{-1} or 8.03 THz at room temperature. Thus the theoretical prediction is in accord with the experiment.

In summary, we have explained the anisotropy of optical phonons in superlattices and its relation with the interface modes by precisely taking into account the long-range Coulomb interaction within a microscopic model. We have shown that the behavior of optical phonons in superlattices is quite intriguing and it takes a detailed microscopic model to understand them fully. The predictions of our microscopic model regarding the anisotropy and interface modes are in good agreement with the available experimental data.

We would like to thank M. V. Klein for fruitful discussions. This work was supported by the U.S. Office of Naval Research under Contract No. N00014-81-K-0430 and the University of Illinois Materials Research Laboratory under the National Science Foundation Contract No. NSF-DMR-83-16981.

[1]R. Merlin, C. Colvard, M. V. Klein, H. Morkoç, A. Y. Cho, and A. C. Gossard, Appl. Phys. Lett. **36**, 43 (1980).

[2]C. Colvard, R. Merlin, M. V. Klein, and A. C. Gossard, Phys. Rev. Lett. **45**, 298 (1980).

[3]J. L. Merz, A. S. Barker, Jr., and A. C. Gossard, Appl. Phys. Lett. **31**, 117 (1977).

[4]A. S. Barker, Jr., J. L. Merz, and A. C. Gossard, Phys. Rev. B **17**, 3181 (1978).

[5]S. K. Yip and Y. C. Chang, Phys. Rev. B **30**, 7037 (1984).

[6]A. Kobayashi, Ph.D. thesis, University of Illinois at Urbana-Champaign, 1985 (unpublished).

[7]T. Toriyama, N. Kobayashi, and Y. Horikoshi, Jpn. J. Appl. Phys. Part 1 **25**, 1895 (1987).

[8]J. P. Mathieu and L. Couture-Mathieu, J. Phys. Radium **13**, 271 (1952).

[9]C. A. Arguello, D. L. Rousseau, and S. P. Porto, Phys. Rev. **181**, 1351 (1969).

[10]S. M. Rytov, Zh. Eksp. Teor. Fiz. **29**, 605 (1956) [Sov. Phys. JETP **2**, 466 (1956)].

[11]E. P. Pokatilov and S. L. Beril, Phys. Status Solidi (b) **118**, 567 (1983).

[12]A. K. Sood, J. Menedez, M. Cardona, and K. Ploog, Phys. Rev. Lett. **54**, 2111, 2115 (1985).

[13]K. Kunc, Ann. Phys. (Paris) **8**, 319 (1973–1974).

[14]K. Kunc, M. Balkanski, and M. Nusimovici, Phys. Status Solidi (b) **72**, 229 (1975).

[15]M. Ilegems and G. L. Pearson, Phys. Rev. B **1**, 1576 (1970).

[16]M. Born and K. Huang, *Dynamical Theory of Crystal Lattices* (Oxford Univ. Press, Oxford, 1956).

[17]A. A. Maradudin, E. W. Montroll, G. H. Weiss, and I. P. Ipatova, in *Solid State Physics: Advances in Research and Applications,* edited by H. Ehrenreich, F. Seitz, and D. Turnbull (Academic, New York, 1971), 2nd ed., Vol. 26, Suppl. 3.

[18]G. Venkataraman, L. A. Feldkamp, and V. C. Sahni, *Dynamics of Perfect Crystals* (MIT Press, Cambridge, MA, 1975).

[19]S.-F. Ren, H.-Y. Chu, and Y.-C. Chang, unpublished.